Thermal conductivity in copper

Dan Marrinan and Sam Stuard

The Ohio State University, Department of Physics, Columbus, OH 43210

Summary
Heat transfer is a very broad topic that is used in many modern day applications including power generation, internal combustion engines, heating and cooling systems, and computers. The temperature of a material can greatly impact its function. Thus, there is a large incentive to develop models that can accurate predict the temperature distribution on an object based on its thermal environment. In this experiment a one dimensional heat conduction model was tested on an insulated copper rod subjected to the initial condition U(x,t=0) = Kx and the boundary conditions U(x=0,t) = U(x=L,t) = 0. This model proved to be fairly accurate, although an inability to subject the rod to the exact conditions used to solve the heat equation produced some inaccuracies. There were also some conditions that caused other modes of heat transfer to be relevant and reduced the accuracy of the one dimensional model's accuracy.

Temperature is a measure of the random thermal motion of the particles that make up a system. Heat conduction takes place when particles with a higher temperature collide with and transfer energy to particles with a lower temperature. Fourier's Law states that the heat current density in one dimension is

$$W = -k\nabla T = -k\frac{dT}{dx}. \quad (1)$$

Here W is the thermal current density, k is the thermal conductivity, T is the temperature, and x the spatial position along the bar [1]. The thermal current density is the heat energy transferred per unit area per unit time. Thermal conductivity is an intrinsic property that measures how quickly heat can be transferred within a material.

Heat in metals is conducted by electrons and phonons [2]. Electrons in a conductor are mobile. Thus when a conductor is subjected to a one dimensional thermal gradient the electrons at the hot end of a conductor diffuse towards the cold end of the conductor and vice versa. As the hot electrons diffuse down the length of the conductor they transfer energy to other particles within the conductor. This decreases the energy of the hot electrons and increases the energy of the rest of the particles in the conductor. Vibrations of the crystal lattice of a solid form waves of energy called phonons [3]. Phonons can be generated by collisions of electrons with particles in the crystal lattice. Thus if there is a net movement of electrons in one dimension, a large number of phonons can be generated in that direction and add to the net heat transfer. Electrons in insulators are not mobile so heat is transferred only via phonons [4].

An equation that models heat conduction can be found by applying conservation of energy to a finite volume as is shown in Appendix A1 in Figure A1. Because one dimensional heat conduction was modeled, heat energy could only be conducted through the flat faces of the volume element in figure B1. No heat was generated within the material in this experiment so any change in energy was due to solely to this heat conduction. The thermal current density can also be written

as the product of the specific heat, mass density, and the rate of change of the Temperature. By equating these two terms and using Fourier's Law it can be shown that

$$\frac{\delta U(x,t)}{\delta t} = \alpha^2 \frac{\delta^2 U(x,t)}{\delta x^2}. \quad (2)$$

A more detailed derivation of this equation can be found in Appendix A1. U designates the temperature difference between the temperature at a position x and the temperature at x=0. By applying the boundary conditions U(0,t) = U(L,t) = 0 and the initial condition U(x,0) = Kx, an expression for the Temperature at a specified time t and position along the bar x can be found to be

$$U(x,t) = -\frac{2KL}{\pi} \sum_{n=1}^{\infty} \frac{(-1)^{\mathrm{n}}}{\mathrm{n}} \sin\left(\frac{n\pi x}{L}\right) e^{-\left(\frac{n^2\pi^2\alpha^2}{L^2}\right)t}. \quad (3)$$

The purpose of this experiment was to test the validity of this expression. The initial conditions and boundary conditions were generated by the experimental setup used in this experiment. A more detailed derivation of this equation can be found in Appendix A2.

Thermocouples consist of two different metals that are connected together and are used to make temperature measurements. They take advantage of the Seebeck effect to measure a difference between two points. This potential difference can then be used to estimate temperature [5]. Figure 1a shows a typical thermocouple made from metals 1 and 2. T_L and T_H refer to high and low temperature junctions between the two metals. If points A and B are held at the same temperature, the potential difference between them, $V_{AB,}$ can be used to calculate the relative temperature $T_L - T_H$. The electrical current density is the charge per unit area per unit time. The electrical current density of a metal that is subjected to a temperature gradient is

$$J = \sigma E - \sigma S \frac{dT}{dx}. \quad (4)$$

J is the electrical current density, σ is the electrical conductivity, E is the electric field, S is the Seebeck coefficient, and $\frac{dT}{dx}$ is the temperature gradient [4].

A concentration gradient of electrons is formed when a temperature gradient is applied to a metal [6]. The electrons at the hot end of the metal gain energy relative to those at the cold end of the metal. The increased energy of the electrons at the hot end also increases their velocity relative to the electrons at the cold end. Electrical conductivity is proportional the velocity of an electron. Therefore the electrons at different temperatures diffuse through the metal at different rates. The Seebeck coefficient is dependent on this difference in the rates of diffusion of hot and cold electrons. Like σ, S is specific to each type of metal. S is also temperature dependent.

The concentration gradient of electrons that is formed causes an imbalance of charge at the two ends of the metal. An electric field is generated within the metal until the two terms in (1) cancel and the current goes to 0. By separating variables and integrating one finds the potential difference between the hot and cold end of the metal. Metals 1 and 2 in Figure 1a have different Seebeck coefficients S_1 and S_2. The potential difference formed between points A and B is

$$V_{BA} = \int_{T_L}^{T_H} (S_2 - S_1)\, dT. \quad (5)$$

This potential difference is found by adding the potential differences between the ends of each section of metal. A more in depth derivation of this potential difference is given in Appendix A3.

As was mentioned before, the Seebeck coefficients are temperature dependent. Often metals in thermocouples are used in temperature ranges where their Seebeck coefficients are essentially constant. The voltage generated is then proportional to the temperature difference between T_H and T_L. T_L is traditionally kept at 0 °C so that the voltage across the thermocouple is proportional to temperature of T_H in degrees Celsius. The thermocouple setup used in this experiment is shown in Figure 1b. This thermocouple setup has only a high temperature junction. The type of thermocouple is specified along with the temperature at the end of the thermocouple. The potential difference that would have been generated in metal 2 between this temperature and 0 °C is then added to the voltage measured by the data acquisition system. This method is called cold junction compensation [7].

The apparatus used for this experiment is shown in Figure 2. A solid copper bar with a diameter of 0.75" was surrounded by 2 inch thick sheets of Styrofoam insulation, and then placed in a wooden box. The ends of the copper bar were joined to 1" copper pipe to form the shape of an H. Plastic tubing was used to bring cold water from a spigot to the inlets of the copper piping at both ends of the bar. Tubing was also used to take water from the outlets of the copper piping to a drain.

This pipe was connected to 1" plastic tubing. This tubing led from a spigot to the bar and from the bar to a drain. Two valves were places at the ends of the copper pipe on one side of the copper bar to allow water to be trapped in that pipe. An electric heater was then attached to the copper pipe at this same end of the copper bar so that the trapped water could be heated. This heated water was then used to heat the copper bar.

11 type T thermocouples were soldered to the copper bar at 3 inch intervals. A type T thermocouple is made up of copper and constantan. Constantan is a copper-nickle alloy [8]. Between 0-100 degrees Celsius type T thermocouples have an error of approximately $\pm$ 1° Celsius [9]. The thermocouples used in this experiment were connected to a National Instruments NI USB-9213 thermocouple input module. The LabView Signal Express software was used to record the temperatures acquired by the NI USB-9213. The NI USB-9213 utilized cold junction compensation to calculate temperature.

Each set of data collected for this experiment was taken over a 3 hour period. First the data acquisition system would be turned on. It took the NI USB-9213 approximately 15 minutes to warm up [10], and it took approximately 20 minutes for the LabView Signal Express software to start. Next the spigot would be opened so that water would begin flowing through both sides of the system. Almost immediately afterwards water would be trapped using the valves on one side of the copper bar. The electric heater would then be turned on to begin heating the trapped water. Thus the initial condition of a linear temperature gradient across the bar was formed by heating one end of the bar and cooling the other. Initially an electronic heater with a thermostat was used to quickly raise the temperature of the hot end of the bar. Normally by the time the approximate temperature target was reached the data acquisition system would be up and running. The thermostat heater was then exchanged for a variable control heater. The variable control heater allowed the hot end of the bar to be kept at a more consistent temperature. Once the hot end of the bar reached the desired temperature the system was allowed to reach steady state. Once the system reached steady state the valves at the hot end of the bar were opened and cold water was al-

lowed to flow by both ends of the pipe. This cold flow enforced the boundary conditions U(0,t) = U(L,t) = 0. A plot of a typical data set for all 11 thermocouples over the duration of an entire experiment is shown in Figure 3a.

The function being validated in this experiment was

$$U(x,t) = T(x,t) - T(0,t). \quad (4)$$

Therefore, it was important to understand how temperature measurements varied between thermocouples. For this reason the room temperature measurements were made of the copper bar before any water was put through the system. The temperatures from all 11 thermocouples averaged, and the standard deviation was computed for each room temperature measurement that was made. The standard deviation for each room temperature measurement is shown in Figure 3b. The maximum standard deviation was found to be 0.0617. This value was taken to be the error for each temperature difference. This is very small relative to the temperature measurements being made which makes the error bars on the data contained in Figures 3c, 4a, and 4b difficult to see. The errors in absolute temperature being measured are $\pm$ 1 °C for type T thermocouples and $\pm$ 1 °C for the NI USB-9213. However, because only differences in temperature were relevant for this experiment, these were not taken into account.

The temperature at the cold end of the bar was set by the cold water coming from the spigot. The temperature of the hot end of the bar was decided upon before each run. Temperatures for the hot end of the bar were chosen to be 45 °C, 50 °C, 55 °C, and 75 °C so that they heat equation could be studied for different sized temperature gradients. The data at time t=0 was fit for each of these curves, giving the values of K for each temperature gradient. For the 45 °C case K = 0.4405 °C/cm; for the 50 °C case K = 0.4919 °C/cm; for the 55 °C case K = 0.5717 °C/cm; for the 75 °C case K = 0.8100 °C/cm. Once K was calculated for each case MATLAB was used to calculate the Fourier Series listed in (6) up to 20 terms. The exponential term is dependent on $-n^2$. Thus by the twentieth term each term was being multiplied by $e^{-400} = 1.9152*10^{-174}$. This sum did not need to be carried out to that many terms, but it added little processing time and was done just to ensure accuracy.

Once U(x,t) was calculated for each case, the fit needed to be transformed in a way that it could be compared to the experimental data. The y-intercept of the linear fit was added to each value in the fit. This was equivalent to adding U(0,0) to each point in the fits. This provided a fairly good fit for the 50 °C case, but the other fits were consistently lower than the experimental data. The thermocouples at the two ends were not completely flush with the ends of the copper bar. Thus the heat would need to be conducted through more copper to get to the boundary conditions than were used to derive (6). An extra 1.5 inches were added to the L used in (6) and the fits were recomputed. These fits are shown in Figure 4a. However, as can be seen especially clearly in the data for t = 60 min, the temperature at the boundaries continued to drop throughout the experiment. This can also be seen in Figure 3a. At the time the cold water was run through both sides the temperature of the last thermocouple can be seen rising and then decaying exponentially like the rest of the thermocouples. This behavior demonstrated that the assumption of constant boundary conditions used to develop (6) were incorrect. Another fit was made adding U(x=0,t) to each point in the length corrected fit. This is shown in Figure 4b. One problem with this fit was that the values of U(x = 0,t = 1 min) and U(x = 0,t = 4 min) were above the y-intercept of the fit for U(x = 0, t = 0). This made it appear that parts of the bar should have actually gained heat af-

ter the cooling process began. However, it did match data for later times more closely and gave insight into the steady state behavior of the bar.

Figure 4b shows that at t = 60 minutes the bar should have had a uniform temperature. However, the data clearly shows that the center of the bar was cooler than the ends of the bar. It was then determined that one dimensional effects were insufficient to describe the long term behavior of the bar. The heat rates of radiation and radial conduction were then compared to the heat rate of one dimensional conduction to determine the relative impact they would have on heating the center of the bar.
The impacts of radiative heat transfer are shown in Appendix A4. Radiation is proportional to temperature to the fourth power. Radiative heat transfer was originally ignored in this experiment because it was thought that the temperature difference between the copper bar and the rest of the room would be too small to be significant compared to the one dimensional heat transfer along the bar. For the areas of the bar that were at a low temperature this proved to be true. However, for the 75 °C case the radiative heat transfer at the end of the bar was approximately 7% of the one dimensional heat transfer. This caused the temperature gradient to be larger in the hot end of the bar than in the cold end of the bar at t = 0 min. This gave the fit an artificially high slope, drove down the y-intercept, and was partly responsible for the problems with the second corrective fit seen in Figure 4b. Once the bar cooled down significantly the radiative heat transfer was 110% of the one dimensional heat transfer. The difference in temperature between the bar and the room was large enough that a steady state condition was reached where the center of the bar remained approximately 3 °C higher than the ends.

Calculations for radial heat transfer are given in Appendix A4. The relatively low heat conduction coefficient of Styrofoam relative to copper made radial heat transfer much less efficient than one dimensional heat transfer for most of this experiment. Even at the hottest part of the bar in the 75 °C case, radial heat transfer was only 3% as large as one dimensional heat transfer. However, after long periods of time when the bar was in steady state the temperature difference between the Styrofoam at room temperature and the Styrofoam touching the bar was so much larger than the temperature difference between the middle and ends of the bar that radial heat transfer was approximately 70% of the one dimensional heat transfer.

This experiment showed that a one dimensional model of heat conduction can be effective predictive tool for an insulated copper bar. However, the curve fitting done showed the importance of the correct application of boundary conditions. Inaccuracies in the solutions to the heat equation came from the distance between the outside thermocouples and the actual ends of the bars as well as the instability of the temperatures at the boundary of the bar. This experiment also demonstrated that other forms of heat transfer can have large effects if the temperature gradients are large enough. Radiation proved to have an impact on the behavior of the bar at high temperatures. Both radiation and radial conduction proved significant when the temperature difference with the bar's surroundings was much larger than the temperature difference between the middle of the bar and the cold water at its ends.

References

1. Y. Dubi and M. Di Ventra, Fourier's law: Insight from a simple derivation. *Physical Review E* **79**, 042101 (2009).
2. P.G. Klemens, Heat conduction in solids by phonons. *Thermochimica Acta*, **218**, 241-255 (1993).
3. W.R.G. Kemp, P.G. Klemens, R.J. Tainsh, and G.K. White,The electrical and thermal conductivities of brasses at low temperatures. *Acta Metallurgica* **9**, 966-968 (1961).
4. R.G. Chambers, Thermoelectric effects and contact potentials. ***Phys. Educ.* 12,** 374 (1977).
5. M. Genix, P. Vairac, and B. Cretin, Local temperature surface measurement with intrinsic thermocouple. *International Journal of Thermal Sciences* **48**, 1679–1682 (2009).
6. V.A. Drebushchak, The Peltier Effect. *Journal of Thermal Analysis and Calorimetry* **91**, 311–315 (2008).
7. J. Williams, Clever techniques improve thermocouple measurements. *EDN* **33**, 145 (1988).
8. M.R. Boudry, A simple conversion formula for type 'T' (copper-constantan) thermocouple readings. *Journal of Physics E: Scientific Instruments* **9**, 1064-1065 (1976).
9. D.L. Don Dowell, A Critical Look at Type T Thermocouples. *International Journal of Thermophysics*, **31**,1527-1532 (2010).
10. National Instruments. User guide and specifications NI USB-9213. (2008).

Figure Captions:

Figure 1: Diagram of Thermocouples. (a) Thermocouple with a cold junction. (b) Modern day thermocouple that would be used with a data acquisition system with cold junction compensation.

Figure 2: Experimental Setup. Shows data acquisition system with 11 thermocouples soft soldered to copper bar in 3 inch increments. Pipes on end allow the flow of water to enforce boundary conditions. Valves on left hand side allow water to be trapped so that end of the bar can be heated.

Figure 3: Uncorrected Data and Fits. (a) Thermocouple data for an entire experiment. The first 2000 seconds show the bar cooling on one side and heating on the other side. At approximately 1000 seconds the switch from the thermostat heater to the variable control heater can be seen. From 2000-5000 seconds the system is approaching steady state. At approximately 5000 seconds the cold water was allowed to flow by both sides of the copper bar. Exponential decay of the temperature can be seen for all thermocouples. An increase in temperature for the coldest temperatures can be seen and were believed to have been caused by the hot exhaust from the hot end of the bar traveling too close to the piping for the cold end and heating it up. A temperature spread of approximately 3 degrees can be seen even at 10000 seconds. (b) Shows standard deviation versus time for several measurements of room temperature. The max of these values was used to find the error on temperature measurements. (c) Original fit of data.

Figure 4: Corrected Fits. (a) Corrected fit using an extra length of 1.5 inches of copper. (b) Corrected fit using the extra length of copper as well as U(0,t) to shift from U(x,t) to T(x,t) instead of using the y-intercept from the linear fit.

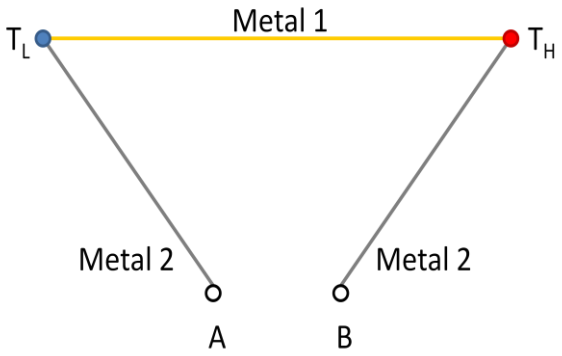

Figure 1a

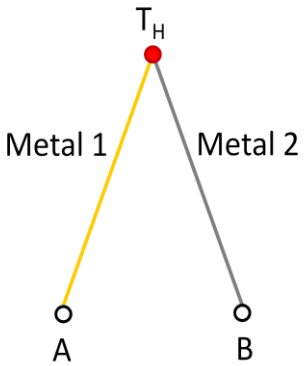

Figure 1b

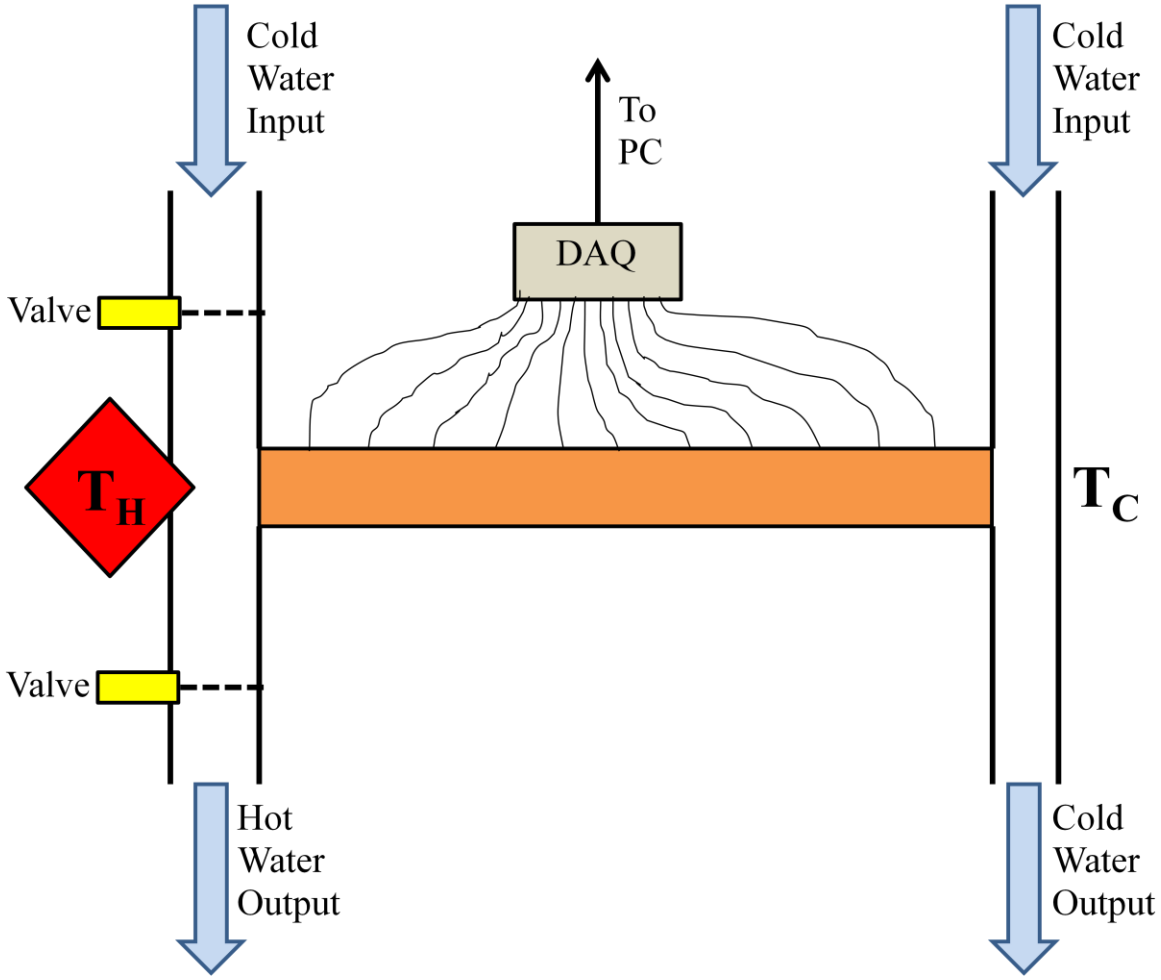
Cold
Water
Input
To
PC
Cold
Water
Input
DAQ
Valve
T_H
T_C
Valve
Hot
Water
Output
Cold
Water
Output

Figure 2

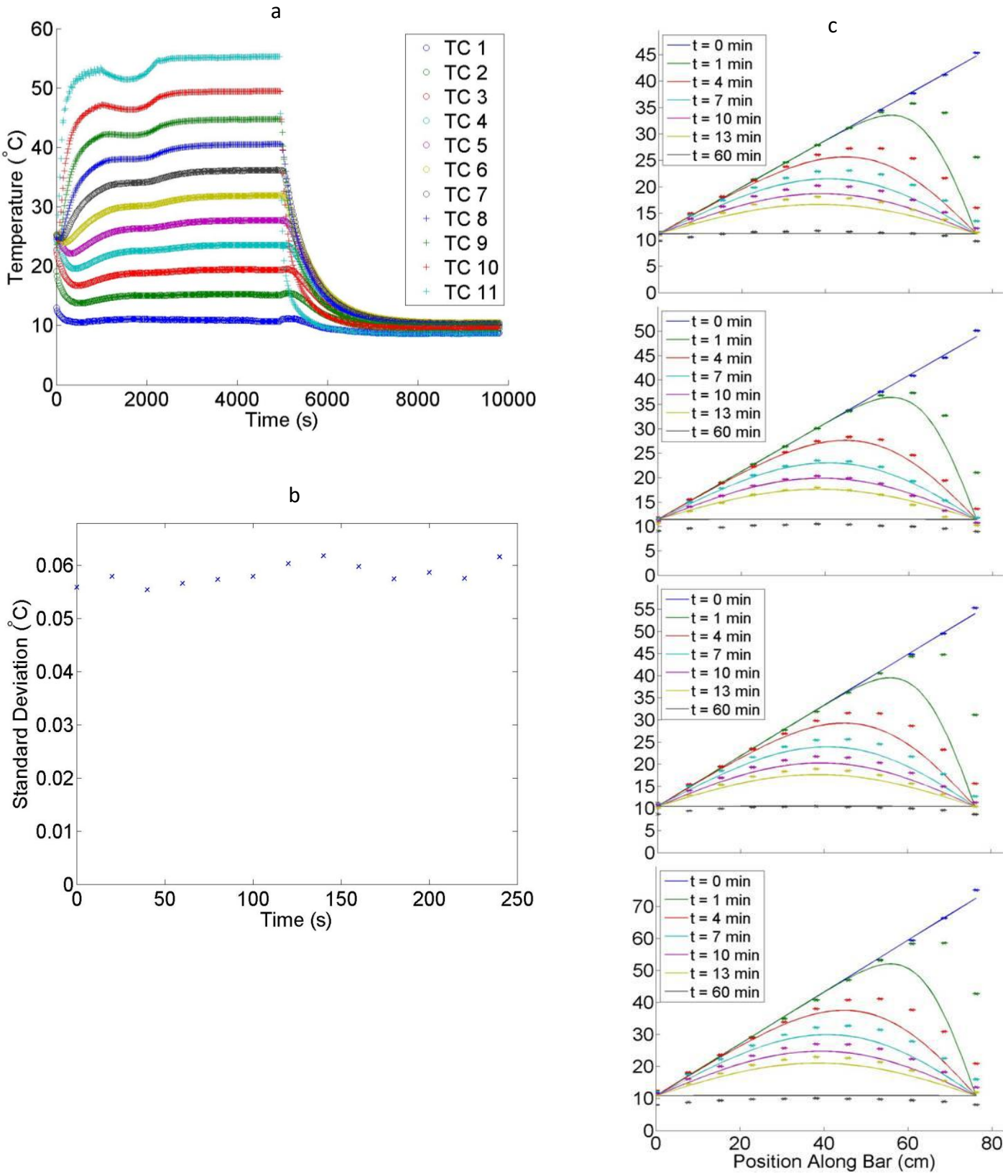
a
Temperature (°C)
Time (s)
TC 1
TC 2
TC 3
TC 4
TC 5
TC 6
TC 7
TC 8
TC 9
TC 10
TC 11
b
Standard Deviation (°C)
Time (s)
c
t = 0 min
t = 1 min
t = 4 min
t = 7 min
t = 10 min
t = 13 min
t = 60 min
Position Along Bar (cm)

Figure 3

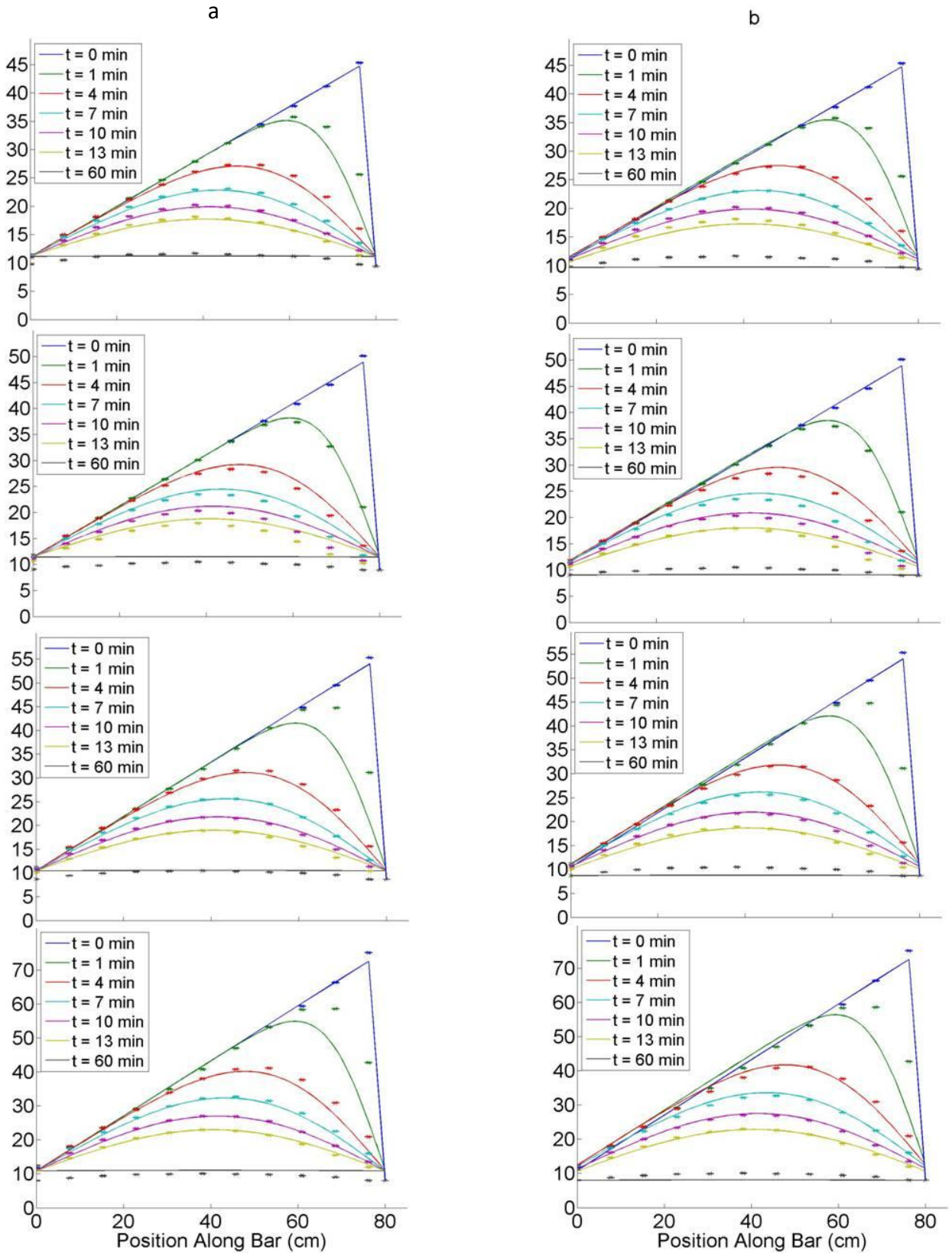
a
b
t = 0 min
t = 1 min
t = 4 min
t = 7 min
t = 10 min
t = 13 min
t = 60 min
Position Along Bar (cm)

Figure 4

Appendix A: Derivations of Important Equations

A1: Derivation of the heat equation

The following quantities were defined for the cylindrical element pictured in Figure A1:

$U(x,t) = Temperature\ at\ a\ given\ distance\ and\ time\ along\ the\ element$
$e(x,t) = Thermal\ energy\ density$
$W(x,t) = Thermal\ current\ density\ (heat\ flux)\ through\ the\ element$
$Q(x,t) = Heat\ generated\ in\ the\ element$
$s(x) = Specific\ heat$
$\rho(x) = mass\ density$

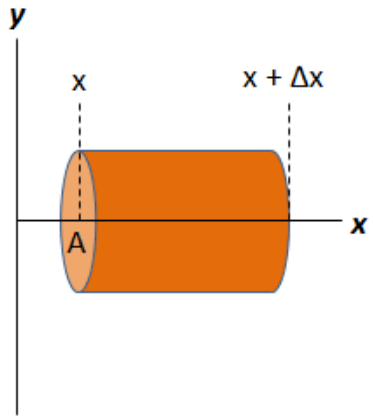

Figure A1. A sample element of the copper bar with length Δx and cross-sectional area A for calculation purposes.

The heat energy stored in the element is

$$e(x,t)A\Delta x = s(x)U(x,t)\rho(x)A\Delta x. \tag{A1}$$

We divide by AΔx to get

$$e(x,t) = s(x)U(x,t)\rho(x). \tag{A2}$$

Conservation of energy yields

$$\frac{\delta}{\delta t}[e(x,t)A\Delta x] = W(x,t)A - W(x+\Delta x,t)A + Q(x,t)A\Delta x. \tag{A3}$$

Substituting in (A2) gives

$$\frac{\delta}{\delta t}[s(x)U(x,t)\rho(x)A\Delta x] = W(x,t)A - W(x+\Delta x,t)A + Q(x,t)A\Delta x. \tag{A4}$$

Assuming that no heat is generated in the element, then $Q=0$ and

$$s(x)\rho(x)\frac{\delta U(x,t)}{\delta t} = \lim_{\Delta x\to 0}\left[\frac{W(x,t) - W(x+\Delta x,t)}{\Delta x}\right]. \tag{A5}$$

The limit turns into a derivative and the expression becomes

$$s(x)\rho(x)\frac{\delta U(x,t)}{\delta t} = -\frac{\delta W(x,t)}{\delta x}. \tag{A6}$$

According to Fourier's Law the thermal current density is

$$W(x,t) = -k\frac{\delta U(x,t)}{\delta x}. \tag{A7}$$

Substituting (A7) into (A6) gives

$$s(x)\rho(x)\frac{\delta U(x,t)}{\delta t} = -\frac{\delta}{\delta x}\left[-k\frac{\delta U(x,t)}{\delta x}\right]. \tag{A8}$$

It is assumed that density, specific heat, and thermal conductivity are constant. The thermal diffusivity is defined as

$$\alpha^2 = \frac{k}{s\rho} \tag{A9}$$

The heat equation is

$$\frac{\delta U(x,t)}{\delta t} = \alpha^2\frac{\delta^2 U(x,t)}{\delta x^2}. \tag{A10}$$

A2: Solution to the heat equation

At time *t=0* we have a linear temperature gradient as our initial condition, so

$$U(x,0) = f(x) = Kx. \tag{A11}$$

For our boundary conditions we have cold water as our reference temperature of *U=0* so

$$U(0,t) = U(L,t) = 0. \tag{A12}$$

Separation of variables will be used so it is assumed that

$$U(x,t) = X(x)T(t). \tag{A13}$$

Substituting (A13) into the heat equation gives

$$X(x)T'(t) = \alpha^2 X''(x)T(t). \tag{A14}$$

Next divide both sides by X(x) and T(t) to get

$$\frac{T'(t)}{T(t)} = \alpha^2\frac{X''(x)}{X(x)} = Y(a\ constant). \tag{A15}$$

Thus X(x) must satisfy the differential equation

$$X''(x) = \frac{Y}{\alpha^2}X(x). \tag{A16}$$

If $Y = \mu^2 > 0$, then

$$X(x) = C_1 cosh(\mu x) + C_2 sinh(\mu x). \tag{A17}$$

If the boundary conditions are imposed this yields $C_1 = C_2 = 0$, a trivial solution. If $Y = 0$, then

$$X''(x) = 0. \tag{A18}$$

Solve this differential equation to get

$$X(x) = C_1 x + C_2. \tag{A19}$$

If the boundary conditions are imposed this again yields $C_1 = C_2 = 0$. If $Y < 0$, we define $\frac{Y}{\alpha^2} = -\mu^2$ so

$$X(x) = C_1 cos(\mu x) + C_2 sin(\mu x). \tag{A20}$$

The boundary conditions mandate that $C_1 = 0$ and $\mu L = n\pi$, so

$$\mu_n = \frac{n\pi}{L}. \tag{A21}$$

Setting $C_2=1$ for convenience the function of x is

$$X(x) = Sin\left(\frac{n\pi x}{L}\right). \tag{A22}$$

For $T'(t)=Y\,T(t)$, the solution is the exponential

$$T(t)=C_3\,e^{Yt}. \tag{A23}$$

Setting $\frac{Y}{\alpha^2} = -\mu^2$, multiplying both sides by α^2, and plugging in (A21)

$$Y = -\frac{n^2\pi^2\alpha^2}{L^2}. \tag{A24}$$

So

$$U_n = X_n(x)\,T_n(t) = \mathrm{C}_3 \sin\left[\frac{n\pi x}{L}\right] e^{-\left[\frac{n^2\pi^2\alpha^2}{L^2}\right]t}. \tag{A25}$$

Using the property of superposition says that

$$U(x,t) = \sum_{n=1}^{\infty} U_n = \sum_{n=1}^{\infty} \mathrm{C}_n \sin\left[\frac{n\pi x}{L}\right] e^{-\left[\frac{n^2\pi^2\alpha^2}{L^2}\right]t}. \tag{A26}$$

Imposing the initial conditions gives

$$U(x,0) = \sum_{n=1}^{\infty} \mathrm{C}_n \sin\left[\frac{n\pi x}{L}\right] = f(x). \tag{A27}$$

The half range sine series expansion of f(x) gives

$$C_n = \frac{2}{L}\int_0^L f(x)\ \sin\left[\frac{n\pi x}{L}\right] dx. \tag{A28}$$

At time t = 0 the temperature distribution is linear so

$$f(x) = Kx \tag{A29}$$

Plugging this back in to the expression for $\mathrm{C_n}$ and evaluating the integral gives

$$C_n = -\frac{2KL}{\pi n}(-1)^n \tag{A30}$$

So ultimately the solution is

$$U(x,t) = -\frac{2KL}{\pi}\sum_{n=1}^{\infty}\frac{(-1)^{\mathrm{n}}}{\mathrm{n}}\sin\left(\frac{n\pi x}{L}\right)e^{-\left(\frac{n^2\pi^2\alpha^2}{L^2}\right)t} \tag{A31}$$

A3: Derivation of equations relating to the Seebeck Effect

The electric current density in a conductor with a temperature gradient is

$$J = \sigma E - \sigma S \frac{dT}{dx}. \tag{A32}$$

Where J is the electric current density, σ is the electrical conductivity, E is the electric field, S is the Thermal Power or Seebeck Coefficient, and $\frac{dT}{dx}$ is the temperature gradient. When no electric field is present and a temperature gradient is applied to the metal, the current density is

$$J = -\sigma S \frac{dT}{dx}. \tag{A33}$$

This current will cause a buildup of opposite charges at the two ends of the metal which induce an electric field. The electric field term grows until the two terms in the current density equation are equal and

$$\sigma E - \sigma S \frac{dT}{dx} = 0. \tag{A34}$$

Separating variables and integrating one gets

$$V_{HL} = -\int_0^L E dx = \int_{T_L}^{T_H} S dT, \tag{A35}$$

where V_{HL} is the potential difference between the high temperature end and the low temperature end.

A thermocouple consists of two metals joined together with different Seebeck coefficients as is shown in Figure 1. T_L and T_H refer to low and high temperature regions respectively. The two different metals are referred to as 1 and 2 respectively. A and B are the two points across which the potential difference V is measured. The potential difference between points A and B is

$$V_{BA} = V_{BH} + V_{HL} + V_{LA}. \tag{A36}$$

The total potential difference is then

$$V_{BA} = -\int_{T_H}^{T_{AB}} S_2 dT - \int_{T_L}^{T_H} S_1 dT - \int_{T_{AB}}^{T_L} S_2 dT. \tag{A37}$$

By manipulating the bounds of the various integrals it can be shown that

$$V_{BA} = \int_{T_L}^{T_H} (S_2 - S_1)\, dT. \tag{A38}$$

A4: Three Dimensional Heat Transfer

One dimension heat transfer was modeled in this experiment using the heat equation. In order to examine the effects of radiation and radial heat conduction the bar must be split into small volume elements as shown in Figure A2.

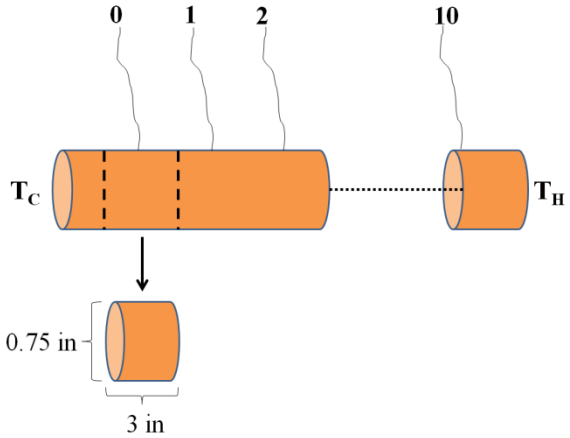

Figure A2. A simplification of the copper bar split into 11 'elements', each with diameter 0.75 in, length 3 in, and one thermocouple per 'element'.

In order to model the radial heat conduction through the Styrofoam and wood, a calculation will be made for each smaller volume for each moment in time. The temperature of each volume will be taken as the temperature of the thermocouple associated with that volume. The temperature of each volume will be highest at the beginning of the experiment so the radial heat conduction will be modeled at t = 0 min using the method of thermal resistance for a composite cylindrical wall with 2 inches of Styrofoam and 1 inch of wood as is shown in Figure A3.

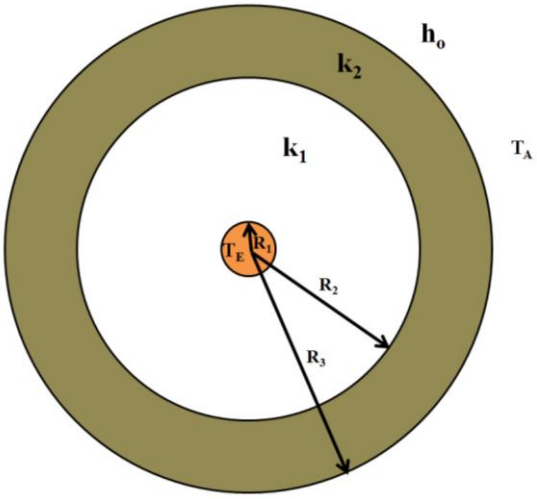

Figure A3. The copper bar is given temperature T_V and radius R_1.The Styrofoam is modeled using its thermal conductivity k_1 and radius R_2. The wood is modeled using its thermal conductivity k_2 and radius R_3. The air outside the box is modeled by its heat transfer coefficient h_O and room temperature.

The radial heat resistance of the Styrofoam is

$$R_{k1} = \frac{\ln(\frac{R_2}{R_1})}{2\pi k_1 L} = 116.8\,\frac{K}{W}, \tag{A39}$$

where k_1 = 0.033 W(m*K). The radial heat resistance of the wood is

$$R_{k2} = \frac{\ln(\frac{R_3}{R_2})}{2\pi k_2 L} = 7.4\frac{K}{W}, \tag{A40}$$

where k_2 = 0.10 W/(m*K). The radial heat resistance of air is

$$R_{ho} = \frac{1}{2\pi R_3 L h_o} = 2.4\frac{K}{W}, \tag{A41}$$

Where h_O = 10 W/(K*m^2). The equation for the thermal current density using the thermal resistance model for a composite cylinder is

$$W = \frac{T_V - T_{Room}}{R_{k1} + R_{k2} + R_{ho}} = \frac{(T_V - 294.5K)}{126.6\frac{K}{W}} \text{ [11].} \tag{A42}$$

The Stefan-Boltzmann Law will be used to model the radiative heat transfer from the cylinder with curved surface area of $A = 2\pi R_1 L$, the Stefan-Boltzmann constant σ, and the emissivity of unpolished copper ε = 0.5. The Stefan-Boltzmann law is

$$P_{net} = A\sigma\epsilon\left({T_V}^4 - {T_{Room}}^4\right) = (1.31 * 10^{-10})\left({T_V}^4 - {T_{Room}}^4\right)$$

Fourier's Law (1) was used to calculate the one dimensional heat conduction along the bar for each volume so that the relative values of different modes of heat transfer could be compared. The results of these calculations are shown in Table A1.

Table A1. Comparison of various methods of heat transfer.

Thermocouple Pair	Axial Conduction (W)	Radial Conduction (W)	Radial Blackbody (W)	Radial-to-Axial Ratio	RadCon-to-AxCon Ratio	RadBla-to-AxCon Ratio
T11-T10	13.11	0.42	1.20	0.12	0.03	0.09
T10-T9	10.44	0.35	1.01	0.13	0.03	0.10
T9-T8	9.14	0.30	0.87	0.13	0.03	0.10
T8-T7	9.49	0.25	0.76	0.11	0.03	0.08
T7-T6	9.24	0.20	0.65	0.09	0.02	0.07
T6-T5	8.79	0.15	0.54	0.08	0.02	0.06
T5-T4	8.74	0.11	0.45	0.06	0.01	0.05
T4-T3	8.57	0.06	0.36	0.05	0.01	0.04
T3-T2	8.54	0.02	0.28	0.04	0.00	0.03
T2-T1	8.79	-0.03	0.21	0.02	0.00	0.02